RSC Advances

Accepted Manuscript

This is an *Accepted Manuscript*, which has been through the RSC Publishing peer review process and has been accepted for publication.

Accepted Manuscripts are published online shortly after acceptance, which is prior to technical editing, formatting and proof reading. This free service from RSC Publishing allows authors to make their results available to the community, in citable form, before publication of the edited article. This *Accepted Manuscript* will be replaced by the edited and formatted *Advance Article* as soon as this is available.

To cite this manuscript please use its permanent Digital Object Identifier (DOI®), which is identical for all formats of publication.

More information about *Accepted Manuscripts* can be found in the **Information for Authors**.

RSC Advances

PAPER

Steam Reforming of Isobutanol for Production of Synthesis Gas over Ni/γ-Al₂O₃ Catalysts

Vimala Dhanala,[a] Sunil K. Maity*,[a] and Debaprasad Shee [a]

The bio-isobutanol has been received widespread attention as bio-fuel, source of chemicals, and synthesis gas in an integrated biorefinery approach. The production of synthesis gas by steam reforming (SR) of isobutanol was investigated in a down-flow stainless steel fixed-bed reactor (FBR) over Ni/γ-Al₂O₃ catalysts in the temperature range of 723-923 K. The NiO/γ-Al₂O₃ catalysts were prepared by wet
10 impregnation method and reduced in the FBR prior to the reaction. The surface area, metal dispersion, crystalline phase, and reducibility of the prepared catalysts were determined using BET, chemisorption, XRD, and TPR respectively. From the TPR study, the maximum hydrogen consumption was observed in the temperature range of 748-823 K for all the catalysts. The presence of nickel species was confirmed by characterizing the catalyst using powder XRD technique. The time-on-stream (TOS) study showed that
15 the catalyst remained fairly stable for more than 10 hrs of TOS. The conversion of carbon to gaseous products (CCGP) was increased with increase in nickel loading on γ-Al₂O₃ and temperatures and decrease in weight hourly space velocity (WHSV). The hydrogen yield was increased with increase in nickel loading on γ-Al₂O₃, WHSV, steam-to-carbon mole ratio (SCMR), and temperature. The selectivity to methane was lowered at higher reaction temperatures and SCMR. The selectivity to CO was decreased
20 with increase in SCMR and decrease in temperature. The work was further extended to thermodynamic equilibrium analysis of SR of isobutanol under the experimental conditions using Aspen Plus and equilibrium results were then compared with experimental results. Reasonably good agreements were observed between trends of equilibrium and experimental results.

1 Introduction

25 The human civilization is deeply reliant on fossil fuels (petroleum, coal, and natural gas) to meet societal needs of energy and chemicals. The fossil fuels resources are however diminishing continuously with increase in exploration to fulfil the growing energy and chemicals requirements due to increase in
30 world population and enhancements of standard of living. The increased usages of fossil fuels also have vast impact on earth environment because of emissions of greenhouse gases (CO₂ and CH₄) which are responsible for global warming. Therefore, there is a strong requirement of finding alternative sustainable sources
35 to meet rising energy and chemical demands of the globe preserving earth environment.

The biodiesel, bioethanol, and bio-*n*-butanol manufactured from biomass have therefore been recognized as promising bio-fuels and have enormous potential to reduce dependency on fossil
40 fuels. The bio-*n*-butanol has been received widespread attention as bio-fuel, source of chemicals, and synthesis gas in an integrated biorefinery approach because of its superior fuel qualities over biodiesel and bio-ethanol.[1-5] The isobutanol having lesser toxicity and higher octane number compared to *n*-butanol

45 and same essential fuel potentials as *n*-butanol is deliberated as one of the promising bio-fuels of the future.[5-6] Bearing in mind the enormous prominence of bio-isobutanol, the steam reforming (SR) of isobutanol derived from biomass was commenced for production of synthesis gas.

50 The catalytic SR of oxygenated hydrocarbons derived from biomass is a propitious technology to produce synthesis gas for applications in chemical industries, for example, in Fischer-Tropsch synthesis of fuels and chemicals.[7] The synthesis gas manufactured by SR is generally subjected to water gas shift
55 reactions (WGSR) to produce high purity hydrogen for applications in fuel cell to generate electricity, transportation fuels, and raw materials in chemical industries.[8] Considering the importance of synthesis gas, the SR of various oxygenated hydrocarbons derived from biomass such as ethanol,[9-13]
60 methanol,[14-16] acetic acid,[17-19] ethylene glycol,[20] dimethyl ether,[21] acetol,[22] *m*-cresol,[23] acetone, ethyl acetate, *m*-xylene, glucose,[24] glycerol,[25-26] fatty acids,[27] and vegetable oils[28-29] were investigated extensively in the past using numerous types of supported metal catalysts in the wide range of temperatures (673-
65 1173K).

A substantial degree of studies have also been devoted on thermodynamic equilibrium analysis of SR,[30] dry reforming,[31]
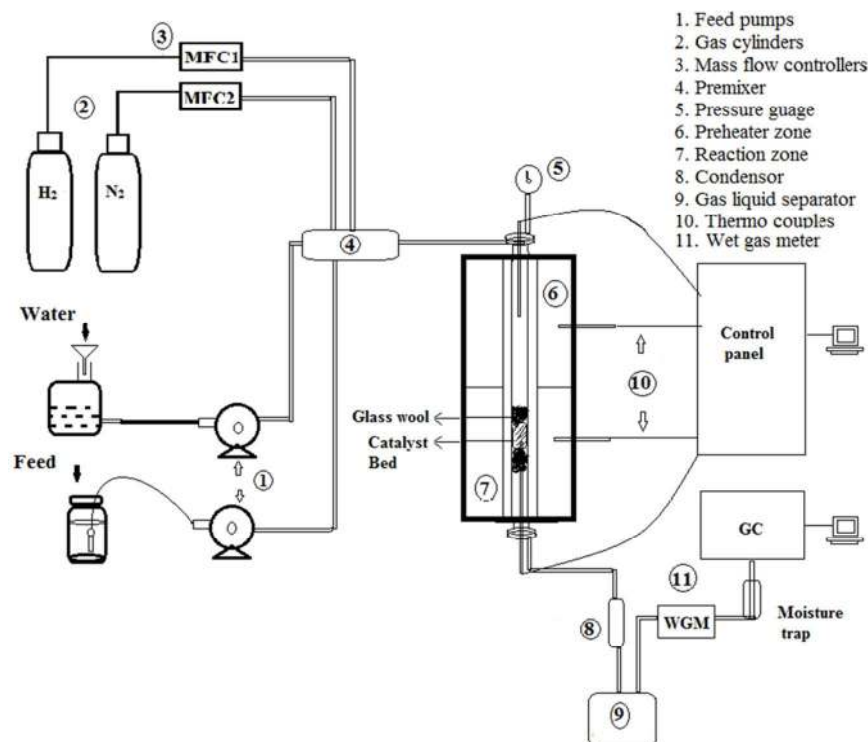
PAPER

Fig. 1 Schematic of the experimental set up.

and sorption enhanced SR,[32-33] and partial oxidation[34] of butanol to predict equilibrium products composition, delineate the effects of various process parameters, and recognize thermodynamically favorable and optimum operating conditions of the process. However, inadequate numbers of experimental investigations are available in open literatures on SR of butanols. Bimbela et al. first reported SR of saturated aqueous solution of *n*-butanol in the temperature range of 823-1023 K in a quartz tubular reactor using Ni/Al$_2$O$_3$ catalysts prepared by co-precipitation method.[35] Cai et al. recently examined the SR of *n*-butanol in the temperature range of 773-873 K using TiO$_2$, CeO$_2$, ZnO supported Co based catalysts.[36] The Co/ZnO catalyst was reported to be most suitable for the SR of *n*-butanol than Co/CeO$_2$ or Co/TiO$_2$. The SR study was then extended to a mixture of *n*-butanol, acetone, and ethanol (6:3:1 mass ratio) corresponding to the product composition of ABE fermentation process using monometallic Co/ZnO and Ir/ZnO and bimetallic Co-Ir/ZnO catalysts. The Co-Ir/ZnO catalysts were found to be most promising catalyst. Cai et al. further extended the work to oxidative SR of bio-*n*-butanol mixture of ABE process using bimetallic Co–Ir/ZnO catalysts.[37] Chakrabarti et al. studied catalytic partial oxidation of isobutanol in absence and presence of steam in a staged millisecond contact time reactor in presence of 1wt%Rh-1wt%Ce/α-alumina catalysts.[38] However, to the best of our knowledge, there is no experimental investigation of SR of isobutanol available in

literatures using nickel supported on γ-Al$_2$O$_3$ catalysts. The inexpensive Ni/Al$_2$O$_3$ catalysts are commercially used for SR of naphtha and hydrocarbons because of high catalytic activity towards breaking of C-C bonds and hence desirable for applications to SR of oxygenated hydrocarbons as well.[39] The present work was therefore commenced to understand the performance of Ni/γ-Al$_2$O$_3$ catalysts for SR of isobutanol.

2 Experimental

2.1 Chemicals

The nickel nitrate hexahydrate (Ni(NO$_3$)$_2$.6H$_2$O) (≥97%) and isobutanol (SG, ≥99%) were purchased from Merck India Limited, Mumbai. The γ-Al$_2$O$_3$ (1/8″ pellets, high surface area, and bimodal) was obtained from Alfa Aesar. All chemicals were used without further purification.

2.2 Catalyst preparation and characterization

The nickel supported on γ-Al$_2$O$_3$ catalysts were prepared by wet impregnation method using nickel nitrate hexahydrate as metal precursor. The NiO supported on γ-Al$_2$O$_3$ catalysts obtained from wet impregnation method were designated as fresh catalysts (NiO/γ-Al$_2$O$_3$) throughout the manuscript. The fresh catalysts were then reduced by hydrogen to obtain Ni/γ-Al$_2$O$_3$ that was designated as reduced catalysts hereafter. The different nickel

RSC Advances

PAPER

Table 1 Mole balance table. [a]

Feed flow rates, mol/hr				Gas products flow rates, mol/hr			
isobutanol	H$_2$O	N$_2$		H$_2$	CO	CH$_4$	CO$_2$
0.052	0.90	0.143		0.406	0.052	0.025	0.108

Liquid products flow rates, mol/hr × 10^3						CBE, %
acetaldehyde	propionaldehyde	2-propenal	butyraldehyde	2-butanone	butanols[*]	
0.01	0.03	0.02	0.03	0.03	3.2	4.9

[a] Conditions- catalyst=20NiAl pellets, T=873 K, SCMR=2.47, WHSV=7.02 h^{-1}.
[*] 1, 2, and iso-butanols.
CBE= carbon balance error.

loaded γ-Al$_2$O$_3$ catalysts, 0, 10, 15, 20, and 25 wt.% nickel on γ-Al$_2$O$_3$ were abbreviated as Al, 10NiAl, 15NiAl, 20NiAl, and 25NiAl respectively.

The surface area and pore volume of both fresh and reduced catalysts were determined using Micromeritics ASAP 2020 phsysorption analyzer. The reducibility and reduction temperature of fresh catalysts were studied using Micromeritics AutoChem II 2920 chemisorption analyzer. The active metal dispersion and metal surface area of the reduced catalysts were determined by hydrogen pulse chemisorption technique using Micromeritics AutoChem II 2920 chemisorption analyzer. Crystalinities present in the catalysts and crystals sizes were determined by powder XRD technique by Phillips X-pert diffractometer using CuKα radiation (λ =1.541Å), 30KV, at a 2θ interval of 10-80° and with a scanning speed of 0.01^0/min.
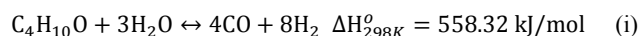
2.3 Experimental setup and procedure

The SR of isobutanol was carried out in a down-flow stainless steel fixed-bed reactor (FBR) in the temperature range of 773-923 K under atmospheric pressure using nitrogen as carrier gas. The schematic of the experimental set up is shown in Fig. 1. The measured amount of catalysts powders diluted with suitable amount of quartz beads were first loaded into the stainless steel reactor (L = 40 cm, OD= 1/2″) supported by two layers of quartz wool on either side of catalyst bed. The reactor was kept inside a tubular furnace and a K-type thermocouple was placed just above the catalyst bed. The temperature of the catalyst bed was controlled within ±1 K by a PID temperature controller. The catalysts were first reduced at 923 K by flowing pure hydrogen through a mass flow controller with a flow rate of 20 ml/min for about 3 hrs to ensure complete reduction of nickel oxide. The reactor was then cooled down to steady state desired reaction temperature under flow of nitrogen gas. The isobutanol and water were then pumped at a desired flow rate using two different metering pumps and vaporized in a pre-mixer maintained at a temperature of 473 K prior to entering into the reactor. The nitrogen, introduced at a specified flow rate using another mass flow controller, served as carrier gas and internal standard for the reaction. The product gas stream was passed through a condenser maintained at 265-273 K to liquefy condensable products present in gas mixture. The cumulative flow rates of non-condensable gas
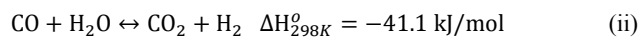
mixtures were recorded with time-on-stream (TOS) using a wet gas meter. Total materials balance was checked for all experimental runs and errors were obtained within ±5%.

The gas samples were analyzed by an online gas chromatography (GC) (Shimadzu GC 2014) equipped with thermal conductivity detector (TCD) using carboseive packed column using argon as carrier gas and calibrated with respect to nitrogen as internal standard. The products of liquid samples were identified by a GC equipped with mass spectrometer (MS) detector and quantified by GC equipped with flame ionization detector (FID) using ZB wax column (30 m×0.25mm×0.25μm) using nitrogen as carrier gas.
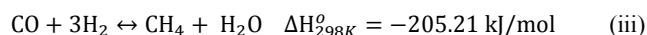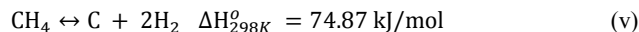
Steam reforming reaction

$$C_4H_{10}O + 3H_2O \leftrightarrow 4CO + 8H_2 \quad \Delta H^o_{298K} = 558.32 \text{ kJ/mol} \quad (i)$$

Water gas shift reaction

$$CO + H_2O \leftrightarrow CO_2 + H_2 \quad \Delta H^o_{298K} = -41.1 \text{ kJ/mol} \quad (ii)$$

Methanation reaction

$$CO + 3H_2 \leftrightarrow CH_4 + H_2O \quad \Delta H^o_{298K} = -205.21 \text{ kJ/mol} \quad (iii)$$

$$CO_2 + 4H_2 \leftrightarrow CH_4 + 2H_2O \quad \Delta H^o_{298K} = -165 \text{ kJ/mol} \quad (iv)$$

Methane decomposition reaction

$$CH_4 \leftrightarrow C + 2H_2 \quad \Delta H^o_{298K} = 74.87 \text{ kJ/mol} \quad (v)$$

CO reduction reaction

$$CO + H_2 \leftrightarrow C + H_2O \quad \Delta H^o_{298K} = -131.29 \text{ kJ/mol} \quad (vi)$$

Boudouard reaction

$$2CO \leftrightarrow C + CO_2 \quad \Delta H^o_{298K} = 172.41 \text{ kJ/mol} \quad (vii)$$
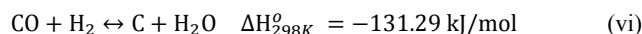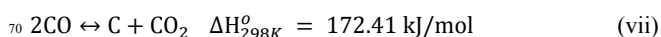
Hydrocarbon dissociation reaction

$$C_nH_{2n+2} \rightarrow nC + (n+1)H_2 \quad \Delta H^o_{298K} = -131.29 \text{ kJ/mol} \quad (viii)$$

Overall reaction

$$C_4H_{10}O + 7H_2O \leftrightarrow 4CO_2 + 12H_2 \quad \Delta H^o_{298K} = 394 \text{ kJ/mol} \quad (ix)$$
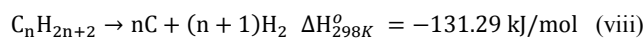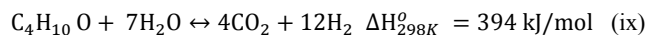
Scheme 1 Chemical reactions involved in steam reforming of isobutanol.

PAPER

Table 2 Characterization of the prepared catalysts.

| Catalysts | BET | | | | Chemisorption | | TPR | Crystallite size by XRD | |
| | Fresh | | Reduced | | | | | | |
	S_{BET}	P_v	S_{BET}	P_v	MD	S_M	T_{max}	Fresh	Reduced
Al	240	0.8	240	0.8	-	-	-	-	-
10NiAl	211	0.7	209	0.74	1.22	8.2	746	8.3	8.9
15NiAl	196	0.6	190	0.67	0.98	6.5	726	10.6	10.4
20NiAl	181	0.5	172	0.58	0.84	5.6	751	12.2	13.8
25NiAl	164	0.5	161	0.54	1.01	6.7	776	15.7	15.3

S_{BET} = surface area, m^2/g; P_v = pore volume, cm^3/g; MD = metal dispersion, %; S_M = metallic surface area, m^2/g metal; T_{max} = maximum reduction temperature.

3 Chemical Reactions

5 The SR of isobutanol is quite complicated in nature involving enormous number of conceivable chemical reactions. Some of the important chemical reactions involved in SR of isobutanol are presented in Scheme 1. The heat of reactions of eqns (ii)-(viii) of Scheme 1 were obtained from the literatures.[31,40] The heat of
10 reaction of eqn (i) and eqn (ix) were calculated using ASPEN plus. The isobutanol reacts with water forming a mixture of hydrogen and carbon monoxide (eqn (i) of Scheme 1). The SR reaction is endothermic in nature absorbing 558.32 kJ/mol of heat. The carbon monoxide then undergoes equilibrium limited
15 WGSR with water forming carbon dioxide and hydrogen (eqn (ii) of Scheme 1). The WGSR is slightly exothermic (ΔH^o_{298K}= -41.1 kJ/mol). The overall SR reaction of isobutanol is endothermic (ΔH^o_{298K} = 394 kJ/mol) (eqn (ix) of Scheme 1). The carbon monoxide and carbon dioxide formed in SR of isobutanol
20 undergo exothermic reaction with hydrogen forming methane and water (eqns (iii)-(iv) of Scheme 1). These reactions are responsible for reduction of hydrogen yield and hence undesirable for SR. The catalyst deactivation due to coke formation is one of the major challenges especially for SR of high
25 molecular weight oxygenated compounds (eqn (viii) of Scheme 1). For nickel catalysts, the formations of five different types of carbons (adsorbed atomic carbon, amorphous carbon, vermicular carbon, bulk nickel carbide, and crystalline graphitic carbon) were reported for SR.[41] The formation carbon occurs by cracking
30 of the C-C bonds of hydrocarbons. Some of the other probable reactions responsible for coke formation are shown by eqns (v)-(vii) of Scheme 1.

4 Results and Discussion

The experiments of SR isobutanol were carried out in a FBR
35 using $Ni/\gamma-Al_2O_3$ catalysts under atmospheric pressure in the wide range of temperatures (773-923 K), steam-to-carbon mole ratios (SCMR) (1-3), and weight hourly space velocities (WHSV) (9.35 -37.43 h^{-1}). The H_2, CO, CO_2, and CH_4 were identified as the non-condensable gaseous products. The two important
40 process variables of SR, SCMR, and WHSV used throughout the manuscript are defined as follows.

$$\text{Steam} - \text{to} - \text{carbon mole ratio (SCMR)} = \left(\frac{\text{rate of moles of water fed}}{\text{rate of moles of isobutanol fed}}\right) / \left(\frac{\text{moles of water}}{\text{moles of isobutanol}}\right)_{stoichiometric} = \left(\frac{\text{rate of moles of water fed}}{7 \times \text{rate of moles of isobutanol fed}}\right) \quad (1)$$

45

$$\text{Weight hourly space velocity (WHSV), } h^{-1} = \frac{\text{total mass flow rate of isobutanol, water, and nitrogen}}{\text{weight of catalyst}} \quad (2)$$

The stoichiometric SCMR used in the definition of eqn (2) was obtained from eqn (ix) of Scheme 1. The definition of SCMR of
50 eqn (1) is useful to represent the extent of surplus (or undersupplied) amount of steam used to that of theoretical requirements. The progress of the SR represented by conversion of carbon to gaseous products (CCGP), hydrogen yield, selectivity to CO, CO_2, and CH_4 are defined as follows.

55

$$\left(\begin{array}{c}\text{Conversion of carbon to}\\\text{gaseous products}\end{array}\right)(CCGP), \% =$$
$$100 \times \frac{\left(\begin{array}{c}\text{rate of moles of carbon present}\\\text{in gaseous products}\end{array}\right)}{(\text{rate of moles of carbon fed})} =$$
$$100 \times \frac{(\text{rate of moles of CO,CO}_2\text{,and methane formed})}{4 \times (\text{rate of moles of isobutanol fed})} \quad (3)$$

$$\text{Hydrogen yield, } \% = 100 \times \frac{\left(\begin{array}{c}\text{rate of moles of}\\\text{hydrogen formed}\end{array}\right)}{\left[\frac{\left(\begin{array}{c}\text{rate of moles of}\\\text{isobutanol fed}\end{array}\right) \times (\text{fractional CCGP})}{\left[\frac{\left(\begin{array}{c}\text{rate of moles of}\\\text{hydrogen formed}\end{array}\right)}{\left(\begin{array}{c}\text{rate of moles of}\\\text{isobutanol reacted}\end{array}\right)}\right]_{stoichiometric}}\right]} =$$
$$100 \times \frac{\left(\begin{array}{c}\text{rate of moles of}\\\text{hydrogen formed}\end{array}\right)}{12 \times \left(\begin{array}{c}\text{rate of moles of}\\\text{isobutanol fed}\end{array}\right) \times (\text{fractional CCGP})} \quad (4)$$

60

$$\text{Selectivity of CO, CO}_2\text{, or CH}_4, \% =$$
$$100 \times \frac{(\text{rate of moles of CO,CO}_2\text{,or CH}_4\text{ formed})}{(\text{rate of moles of CO}_2\text{+CO+CH}_4\text{ formed})} \quad (5)$$

The stoichiometric hydrogen yield used in the definition of eqn (4) was obtained from eqn (ix) of Scheme 1. The definition of
65 hydrogen yield used in the present article is appropriate to judge how far-off the actual hydrogen yield from theoretical maximum hydrogen yield. The analysis of liquid samples by GC-FID and

GC-MS revealed the formation of large number of chemical compounds including acetaldehyde, propionaldehyde, 2-propenal, butyraldehyde, 2-butanone, and butanols (1, 2, and iso-butanols) especially at low CCGP. A representative mole balance table
5 displaying the flow rates of feed, gaseous, and liquid products is shown in Table 1. The catalytic performances for the remaining studies were established based on analysis of gaseous products only.
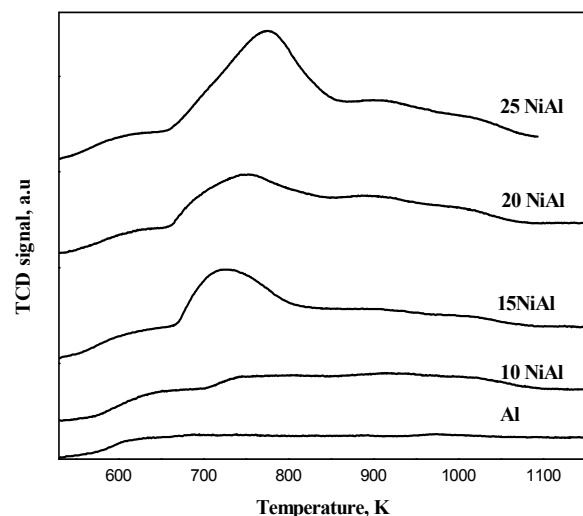
Fig. 2 TPR profiles of fresh catalysts.

4.1 Catalyst characterization

The surface area and pore volume of both fresh and reduced catalysts and metal dispersion and metallic surface area of reduced catalysts are shown in Table 2. The surface area and pore
15 volume of both fresh and reduced catalysts were decreased with increasing nickel loading. With increase in nickel loading, the surfaces of the γ-Al_2O_3 support is covered by increased numbers of nickel crystallites that causes increased coverage of surface of pores leading to decrease in surface area and pore volume. The
20 decrease in surface area may also be due to the difference in atomic weight of nickel and aluminum and blockage of the pores by deposition of nickel during the wet impregnation method. The highest metal dispersion of 1.22% was observed for 10NiAl catalyst.
25 TPR profiles of the fresh catalysts are shown in Fig. 2. The temperature corresponding to the maximum hydrogen consumption (or T_{max}) for the catalysts was observed in the range of 748-823 K. For all the catalysts, the lower reduction temperature peak corresponds to the reduction of bulk NiO
30 reducible species. For higher nickel loading, a small peak appeared at higher temperature (908 K) may be due to the formation of dispersed $NiAl_2O_4$ species which are not detectable by XRD.[42] In all experimental runs, the supported metal oxide catalysts were reduced in FBR at 923 K prior to SR reaction to
35 ensure complete reduction.

The powder XRD results of the fresh and reduced catalysts are shown in Fig. 3. The XRD results of support, γ-Al_2O_3, are also

shown in the same figure. As observed from the figure, the peaks corresponding to 2θ of 45.78 and 66.55^0 were due to Al_2O_3
40 (PDF#821399). The peaks corresponding to 2θ of 37.34, 43.36, and 63.03^0 are due to the presence of nickel oxide species (Fig. 3A) (PDF#731523). The peaks corresponding to 2θ of 44.43, 51.78, and 76.33^0 are due to the presence of nickel species (Fig. 3B) (PDF#870712). The peak corresponding to 2θ of 37.21^0
45 observed for reduced catalyst at higher nickel loadings ($\geq$20%Ni) is due to the bulk NiO species. It was also observed that the sharpness of the nickel peaks was enhanced with increase in nickel loadings. From these results it may be concluded that the nickel remained in dispersed form on high surface area γ-Al_2O_3 at
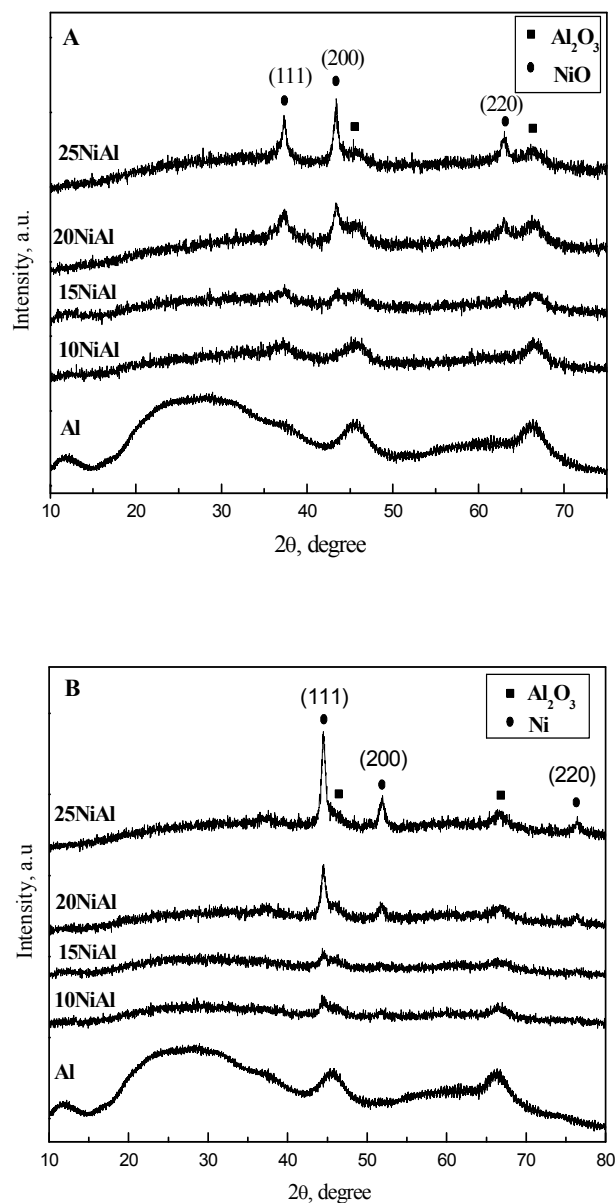50 low nickel loading and nickel crystals started forming with increase in nickel loading.

Fig. 3 Powder XRD patterns of (A) fresh and (B) reduced catalysts.

Table 3 Effects of nickel loading on γ-Al$_2$O$_3$ on CCGP, H$_2$ yield, and selectivity to CO, CO$_2$, and CH$_4$. [a]

Catalysts	CCGP, %	H$_2$ yield, %	Selectivity, %		
			CO	CO$_2$	CH$_4$
Al	0.49	31.67	0	97.63	2.37
10NiAl	31.20	64.49	9.87	64.2	25.93
20NiAl	84.75	65.94	4.54	58.64	36.82
25NiAl	100.00	84.49	5.86	67.4	26.74

[a] Conditions- T=773 K, SCMR=2.49, WHSV=28.25 h^{-1}.

The fresh and reduced catalysts with different nickel loading showed the characteristic nickel oxide/nickel peaks corresponding to (1 1 1), (2 0 0), and (2 2 0) crystal planes. The average crystallite size of nickel and nickel oxide of reduced and fresh catalysts with different nickel loadings respectively were determined using the Scherrer equation from the line widths of the XRD peaks corresponding to (1 1 1), (2 0 0) and (2 2 0) crystal planes as shown in Table 2. The dimensions of nickel and NiO crystallites were in the range 8.3–15.7 nm.
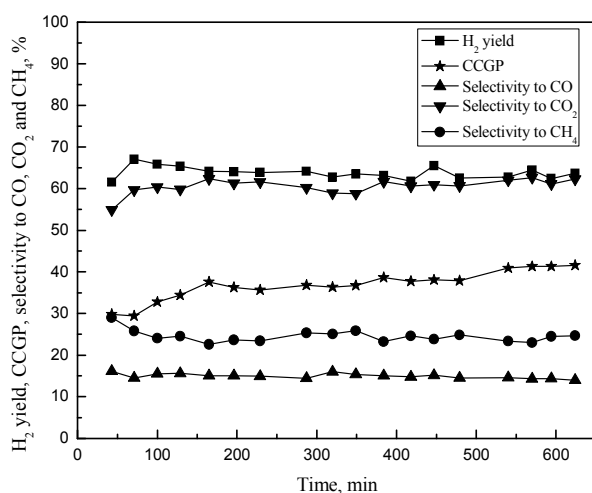
Fig. 4 Time-on-stream behavior of the Ni/γ-Al$_2$O$_3$ catalyst. Conditions: catalyst =15NiAl, T=823 K, SCMR=1.96, WHSV=28.01 h^{-1}.

4.2 Time-on-stream behaviour of 15NiAl

The stability of 15NiAl catalyst for SR of isobutanol was studied for about 10 hrs of TOS at 823 K with SCMR of 1.96 and WHSV of 28.01 h^{-1}. The CCGP, hydrogen yield, selectivity to CO, CO$_2$, and CH$_4$ were stabilized within 150 minutes of TOS as shown in Fig. 4. Beyond 150 minutes, the CCGP and compositions of gaseous products were remained practically constant up to more than 10 hrs of TOS. From this result, it may be concluded that Ni/γ-Al$_2$O$_3$ catalyst is quite stable for SR of isobutanol. For all subsequent experiments, the steady state experimental data were collected after 150 minutes of TOS.

4.3 Effects of weight hourly space velocity

The effects of WHSV were studied over 15NiAl catalyst at 873 K with SCMR of 1.47 as shown in Fig. 5. The CCGP was decreased with increase in WHSV. This is because of decrease of residence time of the reactants and products in the reactor. The hydrogen yield was increased slightly with increase in WHSV. With an

initial increase of WHSV, the selectivity to CO and CH$_4$ were decreased and that of CO$_2$ was increased slightly. However, the selectivity to CO, CO$_2$, and CH$_4$ practically remains unaffected beyond WHSV of ~15 h^{-1}. The identical trends of results were also reported for SR of *n*-butanol[35] and oxidative SR of ethanol.[43] Therefore, the remaining studies were performed with WHSV more than 15 h^{-1} for better comparison of selectivity to CO, CO$_2$, and CH$_4$.
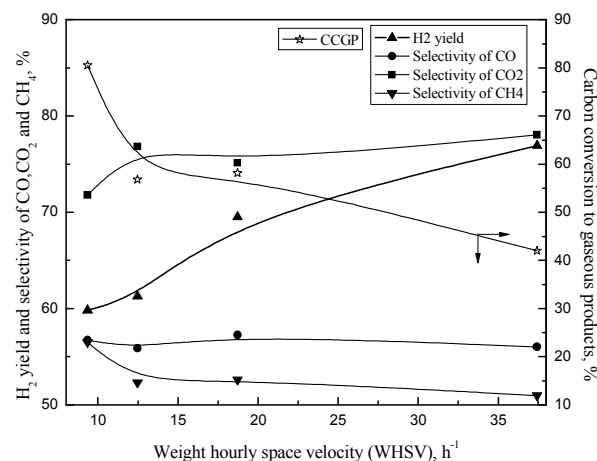
Fig. 5 Effects of WHSV on CCGP, H$_2$ yield, and selectivity to CO, CO$_2$, and CH$_4$. Conditions: catalyst = 15NiAl, T= 873 K and SCMR= 1.46.

4.4 Effects of nickel loading on γ-Al$_2$O$_3$

The three different nickel loaded γ-Al$_2$O$_3$ catalysts, 10NiAl, 20NiAl, and 25NiAl were examined for SR of isobutanol at 773 K with SCMR of 2.49 and WHSV of 28.25 h^{-1}. To delineate the role of the support, SR of isobutanol, the study was also conducted with pure γ-Al$_2$O$_3$ under identical experimental conditions. A very low CCGP was observed with pure γ-Al$_2$O$_3$ suggesting that pure γ-Al$_2$O$_3$ is inactive for SR of isobutanol under the experimental condition. The effects of nickel loading on γ-Al$_2$O$_3$ on CCGP, H$_2$ yield, and selectivity to CO, CO$_2$, and CH$_4$ are shown in Table 3. As observed from the table, the CCGP increases with increase of nickel loading on γ-Al$_2$O$_3$. The increase of catalytic activity with increase of nickel loading on γ-Al$_2$O$_3$ is due to increase in number of active sites in the catalyst. The hydrogen yield was also increased with increase of nickel loading on γ-Al$_2$O$_3$. The maximum hydrogen yield of about 84% was observed with 25NiAl. The selectivity to CO, CO$_2$, and CH$_4$ remained almost unaffected with increase of nickel loading on γ-Al$_2$O$_3$.

4.5 Effects of steam-to-carbon mole ratio

The effects of SCMR on CCGP, hydrogen yield, and selectivity to CO, CO$_2$, and CH$_4$ were studied in the SCMR range of 1.1-3.2 at 873 K over 15NiAl catalysts with WHSV of 18.08 h^{-1} as shown in Fig. 6. About 75% of CCGP was observed under experimental conditions. The hydrogen yield was increased with increase in SCMR as observed from the figure. The maximum hydrogen yield of about 81% was observed with SCMR of 3.2. With increase in SCMR, the increase in selectivity to CO$_2$ and decrease

RSC Advances Accepted Manuscript

in selectivity to CO and CH_4 were observed. With increase in SCMR, the WGSR (eqn (ii) of Scheme 1), butanol (eqn (i) of Scheme 1) and methane (reverse reaction of eqns (iii)-(iv) of Scheme 1) SR reactions increases leading to increase in hydrogen

5 yield and selectivity to CO_2 and decrease in selectivity to CO and CH_4. Hu and Lu also reported similar trends of results for SR of acetic acid over Ni/Al_2O_3 catalyst.[44]
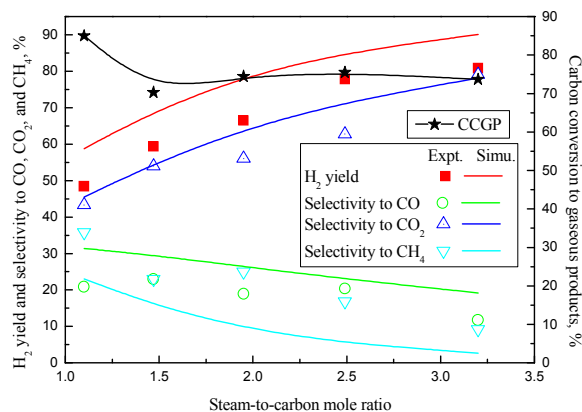

Fig. 6 Effects of steam-to-carbon mole ratio on CCGP, H_2 yield, and
10 selectivity to CO, CO_2, and CH_4. Conditions: catalyst =15NiAl, T=873 K, WHSV=18.08 h^{-1}.

The study was further extended to thermodynamic equilibrium analysis of SR of isobutanol using R-Gibbs reactor with UNIF-LBY as property method using Aspen Plus under the identical
15 experimental conditions. The detailed approach of thermodynamic equilibrium analysis of SR was presented in our earlier publications.[45-46] The results of thermodynamic equilibrium analysis of SR of isobutanol were then compared with experimental data as shown in Fig. 6. The experimental
20 trends of results displayed good agreement with that of thermodynamic equilibrium analysis results. However, the hydrogen yield and selectivity to CO was somewhat lower than that of equilibrium values. The selectivity to CH_4 was observed to be higher than that of equilibrium selectivity. From these results
25 it may be concluded that reactions involved in SR of isobutanol (especially WGSR and methane SR reaction) remained slightly away from the equilibrium under the experimental conditions studied.

4.6 Effects of temperature

30 The effects of temperature on CCGP, hydrogen yield, and selectivity to CO, CO_2, and CH_4 were studied in the temperature range of 773-923 K over 15NiAl catalyst with SCMR of 1.47 and WHSV of 17.0 h^{-1} as shown in Fig. 7. The CCGP was increased with increase in temperature. The endothermic SR reactions (of
35 isobutanol and intermediates) are favorable at higher temperatures that result increase of CCGP with temperature. The hydrogen yield was decreased marginally with increase in temperatures and the maximum hydrogen yield of ~65% was observed at 923 K. The increase of hydrogen yield is due to
40 increase in CCGP and favorable endothermic SR of methane (eqns (iii)-(iv) of Scheme1) at higher temperatures. The increase of selectivity to CO and decrease of selectivity to CO_2 was observed with increasing temperature. A slight decreasing trend

of selectivity to methane with temperatures was also witnessed.
45 The trends of results can be explained by the fact that endothermic SR of isobutanol (eqn (i) of Scheme 1), reverse methanation reaction (eqn (iii)-(iv) of Scheme 1), and reverse WGSR (eqn (ii) of Scheme 1) are favored at higher temperatures. The experimental results of the present study were found to be
50 comparable with SR of oxygenated compounds like acetic acid in presence of Ni/Al_2O_3.[44] Furthermore, the thermodynamic equilibrium analysis of SR of isobutanol was performed at different temperatures under the experimental conditions and the results were then compared with experimental data as shown in
55 Fig. 7. As observed from the figure, the trends of experimental results are in good agreement with equilibrium results. However, the reactions involved in SR of isobutanol are away from the equilibrium to some extent causing somewhat lower hydrogen yield and selectivity to CO and CO_2 and higher selectivity to CH_4
60 compared to equilibrium.
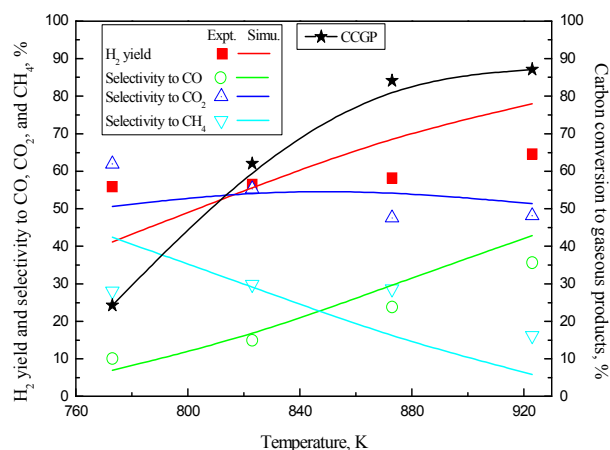
Fig. 7 Effects of temperatures on CCGP, H_2 yield, and selectivity to CO, CO_2, and CH_4. Conditions: catalyst =15NiAl, SCMR=1.46, WHSV=18.72 h^{-1}.

65 **4.7 Optimum conditions**

The optimum process conditions were determined to achieve complete CCGP and maximum hydrogen yield with very low selectivity to methane.[45,46] The CCGP depends on reactivity of the catalysts and WHSV. The catalytic activity on the other hand
70 is a strong function of nickel loading on γ-Al_2O_3 (Table 2). Therefore, the maximum allowable nickel loading on γ-Al_2O_3 (generally 25-30 wt.%) should be used as catalyst with appropriate WHSV to achieve complete CCGP. The hydrogen yield and selectivity to methane depends strongly on SCMR and
75 temperature. With increase of SCMR and temperature, the hydrogen yield increases and selectivity to methane decreases (Fig. 6&7). The high SCMR is also desirable to minimize coke formation on the catalyst. From this discussion it may be apparently concluded that maximum permissible SCMR and
80 temperature should be used to achieve maximum hydrogen yield with low selectivity to methane. However, the operation of SR at high temperature and SCMR will affect the thermal efficiency of the process significantly. Therefore, it may be concluded that optimum process conditions of SCMR= 2.5-3.0 and temperature
85 = ~900 K should be used for SR of isobutanol.[45]

5 Conclusions

The SR of isobutanol was investigated in a down-flow fixed-bed reactor over Ni/γ-Al$_2$O$_3$ catalysts. The NiO/γ-Al$_2$O$_3$ catalysts were prepared by wet impregnation method. The catalysts were characterized by BET, chemisorption, TPR, and powder XRD. The powder XRD revealed the presence of NiO species in the catalysts. The nickel supported on γ-Al$_2$O$_3$ catalysts were quite stable and active for SR of isobutanol. The detailed study was performed to comprehend the effect of various process parameters such as nickel loading on γ-Al$_2$O$_3$, WHSV, SCMR, and temperature on CCGP, hydrogen yield, and selectivity to CO, CO$_2$, and methane. The CCGP was increased with rise in nickel loading on γ-Al$_2$O$_3$ and temperatures. The increase of WHSV resulted in decrease of CCGP. The hydrogen yield was increased with increase in nickel loading on γ-Al$_2$O$_3$, WHSV, and SCMR. The desired low selectivity to methane was favored at higher reaction temperatures and SCMR. The maximum hydrogen yield of about 80% was observed at 873 K with SCMR of 3.2. The thermodynamic equilibrium analysis of SR of isobutanol was carried out using Aspen plus and the results were then compared with experimental data. The trends of experimental results were found to be in good agreement with equilibrium results.

Nomenclatures

BET	Brunauer-Emmett-Teller
CCGP	conversion of carbon to gaseous products, %
T$_{max}$	maximum reduction temperature, K
SCMR	steam-to-carbon mole ratio
FBR	fixed bed reactor
ΔH^o_{298K}	standard heat of reaction at 298 K, kJ/mol
P$_v$	pore volume, cm^3/gm
S$_{BET}$	BET surface area, m^2/gm
TPR	temperature programmed reduction
TOS	time-on-stream
WHSV	weight hourly space velocity, h^{-1}
WGSR	water gas shift reaction

Notes and references

^{a} Department of Chemical Engineering, Indian Institute of Technology Hyderabad, Ordnance Factory Estate, Yeddumailaram-502205, Andhra Pradesh, India.

* Corresponding author (Dr. Sunil K. Maity): Phone: +91-40-2301-6075; Fax: +91-40-2301 6003; E-mail: sunil_maity@iith.ac.in

1. M. Kumar and K. Gayen, *Appl. Energy*, 2011, **88(6)**, 1999-2012.
2. P. Dürre, *Curr. Opin. Biotechnol.,* 2011, **22**, 331-336.
3. B.G. Harvey and H.A. Meylemans, *J. Chem. Technol. Biotechnol.,* 2011, **86(1)**, 2-9.
4. M. Mascal, *Biofuels Bioprod. Biorefin.,* 2012, **6(4)**, 483-493.
5. E.M. Green, *Curr. Opin. Biotechnol.,* 2011, **22**, 337-343.
6. M.R. Connor and J.C. Liao, *Curr. Opin. Biotechnol.,* 2009, **20(3)**, 307-315.
7. J. Xuan, M.K.H. Leung, D.Y.C. Leung and M. Ni, *Renewable Sustainable Energy Rev.*, 2009, **13**, 1301-1313.
8. M. Balat, *Int. J. Hydrogen Energy*, 2008, **33**, 4013-4029.
9. P. Biswas and D. Kunzru, *Int. J. Hydrogen Energy*, 2007, **32**, 969-980.
10. M. Ni, D.Y.C. Leung and M.K.H. Leung, *Int. J. Hydrogen Energy*, 2007, **32**, 3238-3247.
11. V.V. Galvita, G.L. Semin, V.D. Belyaev, V.A. Semikolenov, P. Tsiakaras and V.A. Sobyanin, *Appl. Catal. A.*, 2001, **220**, 123-127.
12. J.Y.Z. Chiou, W. Wang, S. Yang, C. Lai, H. Huang and C. Wang, *Catal. Lett.*, 2013, DOI 10.1007/s10562-013-0975-9.
13. X. Yu, W. Chu, N. Wang and F. Ma, *Catal. Lett.,* 2011, **141**, 1228-1236.
14. D.R. Palo, *Chem. Rev.,* 2007, **107**, 3992-4021.
15. S. Sá, H. Silva, L. Brandão, J.M. Sousaa and A. Mendes, *Appl. Catal. B.*, 2010, **99**, 43–57.
16. G. Wu, D. Mao, G. Lu, Y. Cao and K. Fan, *Catal Lett.*, 2009, **130**, 177–184.
17. J.R. Galdámez, L. García and R. Bilbao, *Energy Fuels*, 2005, **19**, 1133-1142.
18. L. An, C. Dong, Y. Yang, J. Zhang and L. He, *Renewable Energy*, 2011, **36**, 930-935.
19. S. Thaicharoensutcharittham, V. Meeyoo, B. Kitiyanan, P. Rangsunvigit and T. Rirksomboon, *Catal. Today*, 2011, **164**, 257-261.
20. N. Wang, N. Perret and A. Foster, *Int. J. Hydrogen Energy*, 2011, **36**, 5932-5940.
21. K. Takeishi and H. Suzuki, *Appl. Catal.* A , 2004, **260**, 111-117.
22. M.C. Ramos, A.I. Navascués, L. García and R. Bilbao, *Ind. Eng. Chem. Res.*, 2007, **46**, 2399-2406 .
23. C. Wu and R. Liu, *Energy Fuels*, 2010, **24**, 5139-5147.
24. X. Hu and G. Lu, *Appl. Catal. B*, 2009, **88**, 376-385.
25. P.D. Vaidya and A.E. Rodrigues, *Chem. Eng. Technol.*, 2009, **32(10)**, 1463-1469.
26. S. Kitamura, T. Su-enaga, N. Ikenaga, T. Miyake and T. Suzuki *Catal. Lett.*, 2011, **141**, 895-905.
27. C.M. Jeong, G.W. Park, J. Choi, J.W. Kang, S.M. Kim, W. Lee, S. Woo and H.N. Chang, *Int. J. Hydrogen Energy*, 2011, **36**, 7505-7515.
28. M. Marquevich, R. Coll and D. Montané, *Ind. Eng. Chem. Res.*, 2000, **39**, 2140-2147.
29. M. Marquevich, X. Farriol, F. Medina and D. Montané, *Ind. Eng. Chem. Res. ,* 2001, **40**, 4757-4766.
30. G.A. Nahar and S.S. Madhani, *Int. J. Hydrogen Energy*, 2010, **35**, 98-109.
31. W. Wang, Fuel, 2011, **90**, 1681-1688.
32. A.L.D. Silva and I.L. Müller, *Int. J. Hydrogen Energy*, 2011, **36**, 2057-2075.
33. W. Wang and Y. Cao, *Int. J. Hydrogen Energy*, 2011, **36**, 2887-2895.
34. W. Wang and Y. Cao, *Int. J. Hydrogen Energy*, 2010, **35**, 13280-13289.
35. F. Bimbela, M. Oliva, J. Ruiz, L. García and J. Arauzo, *J. Anal. Appl. Pyrolysis.*, 2009, **85**, 204-213.
36. W. Cai, P.R. Piscina and N. Homs, *Bioresour. Technol.*, 2012, **107**, 482-468.
37. W. Cai, N. Homs and P.R. Piscina, *Green Chem.*, 2012, **14**, 1035-1043.
38. R. Chakrabarti, J.S. Kruger, R.J. Hermann and L.D. Schmidt, *RSC Adv.*, 2012, **2**, 2527-2533.
39. J.N. Armor, *Appl. Catal. A*, 1999, **176**, 159-176.
40. J.D. Holladay, J. Hu, D.L. King and Y. Wang, *Catal Today*, 2009, **139**, 244-260.
41. P. Forzatti and L. Lietti, *Catal Today*, 1999, **52**, 165-181.
42. A.J. Akande, R.O. Idem and A.K. Dalai, *Appl. Catal. A*, 2005, **287**, 159-175.
43. P. Biswas and D. Kunzru, *Chem. Eng. J.*, 2008, **136**, 41-49.
44. X. Hu and G. Lu, *Appl. Catal. B*, 2010, **99**, 289-297.
45. S.R. Yenumala and S.K. Maity, *Int. J. Hydrogen Energy*, 2011, **36**, 11666-11675.
46. S.R. Yenumala and S.K. Maity, *J. Renewable Sustainable Energy*, 2012, **4**, 043120.

GRAPHICAL ABSTRACT

The performance of Ni//γ-Al$_2$O$_3$ catalysts was investigated for steam reforming of isobutanol in a down-flow stainless steel fixed-bed reactor in the temperature range of 723-923 K.

Isobutanol   H$_2$O   Synthesis gas

HO   Steam reforming   →   H$_2$+CO+CO$_2$

Ni/γ-Al$_2$O$_3$